Department of Veterans Affairs

Journal of Rehabilitation Research and Development
Vol. 38 No. 2, March/April 2001
Pages 183–190

Intramedullary osseointegration: Development of a rodent model and study of histology and neuropeptide changes around titanium implants

Magnus Ysander, MD; Rickard Brånemark, MD, PhD; Kjell Olmarker, MD, PhD; Robert R. Myers, PhD
VA San Diego Healthcare System; Department of Orthopedics, Gothenburg University, Gothenburg, Sweden

Abstract—A rodent model has been developed to explore intramedullary osseointegration and the phenomena of osseoperception. Osseointegration with endosseous titanium implants is frequently used in oral surgery. More recently, intramedullary osseointegration has been used for direct skeletal anchoring of amputation prostheses, a procedure that provides for a stable prosthesis with improved perception. Experimental, commercially pure titanium rods with threaded ends were surgically implanted in the intramedullary space of 18 rat femurs, and were left in place for 8 wk. Microscopic and immunohistochemical observation of the titanium/bone interface at this time-point indicated successful osseointegration with normal remodeled bone adjacent to the fixture. Calcitonin gene-related peptide activity was upregulated during the process of bone remodeling, and there was no significant inflammatory reaction. There was new, normal bone adjacent to and fully occupying the space between fixture threads. Innervation also appeared normal in remodeled bone, as indicated by immunohistochemical observation of small nerve fibers with the antibody Protein Gene Product 9.5 (PGP 9.5). The model will be used further to explore intramedullary osseointegration and osseoperception in connection to clinical applications.

Key words: *bone, neuropeptides, osseointegration, osseoperception, proprioception.*

INTRODUCTION

The ability to achieve bone anchoring of implants has been of major interest in both oral surgery and orthopedics (1,2). However, direct bone anchoring without intervening soft tissue formation was not accepted as an achievable bioengineering condition until the success of permanent titanium implants for dental prostheses, using the concept of osseointegration (3). Osseointegration is broadly defined as the permanent incorporation of a nonbiological component to carry unlimited functional load in endoprosthetic and exoprosthetic replacement of structure and function (4), and is reserved to identify the surgical procedures and material science that result in permanent attachment of titanium to human bone. In oral surgery, the concept of osseointegration is considered state-of-the-art therapy for edentulism (5,6).

More recently, osseointegration has been extended to orthopedic applications (7). Of particular interest is the treatment of transfemoral amputees where traditional rehabilitation using socket prostheses causes complications related to prosthesis retention and function. Preliminary results with osseointegrated implants (4) indicated that direct skeletal anchoring of prostheses could be achieved using intramedullary implants.

This material is based on work supported by VA Rehabilitation Research and Development and the Göteborg Medical Society, Gothenburg, Sweden (#98/292).

Address all correspondence and requests for reprints to: Robert R. Myers, PhD, Senior Research Career Scientist, VA San Diego Healthcare System (151), 3350 La Jolla Village Drive, San Diego, CA 92161; email:rmyers@ucsd.edu.

One important observation is that patients with osseointegrated prosthesis are able to "feel" through their artificial limb. This heightened perception of sensory stimuli is termed osseoperception (8) and is of great importance because of its ultimate clinical benefit. Patients report improved feedback control of their prosthesis, and this promotes better psychological acceptance of the limb substitute. Quantification of vibratory perception around osseointegrated implants has been assessed in humans by means of a psychophysical threshold determination of passive stimuli applied to the implants, whereby the subject has to answer whether the stimulus is detected or not. The measured perception of vibration in the limb with an osseointegrated prosthesis was generally comparable to that of the normal contralateral limb, and was significantly improved over the threshold level obtained with a conventional amputation prosthesis. These measurements suggest that direct, stable and permanent anchorage of amputation prostheses to the skeleton via osseointegrated fixtures and skin-penetrating abutments is a useful clinical technique that improves the perception of the environment by the amputee.

To explore osseointegration and the anatomical basis of osseoperception, we have developed a model of titanium implantation in the rat femur. This report describes the model and the results of histological and neuropeptide investigations in remodeled bone incorporating osseointegrated intramedullary titanium fixtures.

METHODS

Animals

Eighteen male, adult Sprague-Dawley rats were used in this study. The average weight of the animals at surgery was 286 g; after 8 wk of osseointegration, the average weight was 475 g. This weight gain is normal in healthy male rats. As described below, titanium implants were implanted unilaterally in the medullary cavity of the femur of each animal. The distribution between sides was equal. The contralateral, unoperated femur was used as histological control. For the entire experimental period two or three animals were kept in each cage with an unlimited supply of fresh water and rodent pellets (Harlan Teklad, Madison, WI). The experimental protocol was approved by the San Diego VA Animal Studies Subcommittee and by the Ethical Committee for Use of Laboratory Animals in Gothenburg, Sweden.

Implants

Experimental implants were manufactured from commercially pure titanium, grade 2. The implants had an overall length of 20 mm. An 11.4-mm-long, smooth middle section had a core diameter of 1.5 mm. At each end there was a 4.3-mm-long M2 thread (**Figure 1a**). A 2-mm-deep, hexagonal hole with 1.2-mm diameter was available at the distal end of the implant to facilitate insertion (**Figure 1b**).

The implants were cleaned using oscillating ultrasound equipment after placing them in n-butanol within a glass container. They were processed two times for 10 min each time, with a change of liquid. The objects were then rinsed three times and processed another 10 min in 70 percent ethanol. From this stage, in order not to contaminate the titanium surface, the implants were kept in a dry glass container and were only handled with titanium instruments. Finally, the implants, together with all necessary instrumentation, were moist-sterilized at 134 ˚C for 40 min.

Anesthesia and Surgery Preparation

Animals were anesthetized using a 50 mg/ml solution of ketamin (Ketalar®, Warner Lambert, Ireland) and 5 mg/ml diazepam (Stesolid Novum®, Dumex, Denmark) in a 1:5 proportion. One to 1.2 ml of the mixture was slowly injected intraperitoneally with a 0.6 mm diameter needle. The hindquarter on the experimental side was shaved, and the entire dorsal aspect of the animal was disinfected.

Surgical Technique

Surgery was performed under sterile conditions. Each rat was placed supine with the left knee joint in a maximally flexed position. A 15-mm-long mid-line, longitudinal skin incision was made over the patella. The knee joint capsule was incised longitudinally, 2–3 mm medial to the patella. By lifting the patella gently and moving it laterally, the knee joint was exposed. This maneuver was facilitated by a slight extension of the knee.

The entrance point for drilling through the femoral cartilage surface, central and parallel to the long axis of the femur, was defined. The femoral medullary cavity was opened using a 1.7-mm-diameter hand drill. Initially the drill was angled perpendicular to the cartilage surface to avoid sliding. After perforation of the superficial cartilage layer, the drill inclination was adjusted to correspond to the long axis of the femur. Entering the medullary

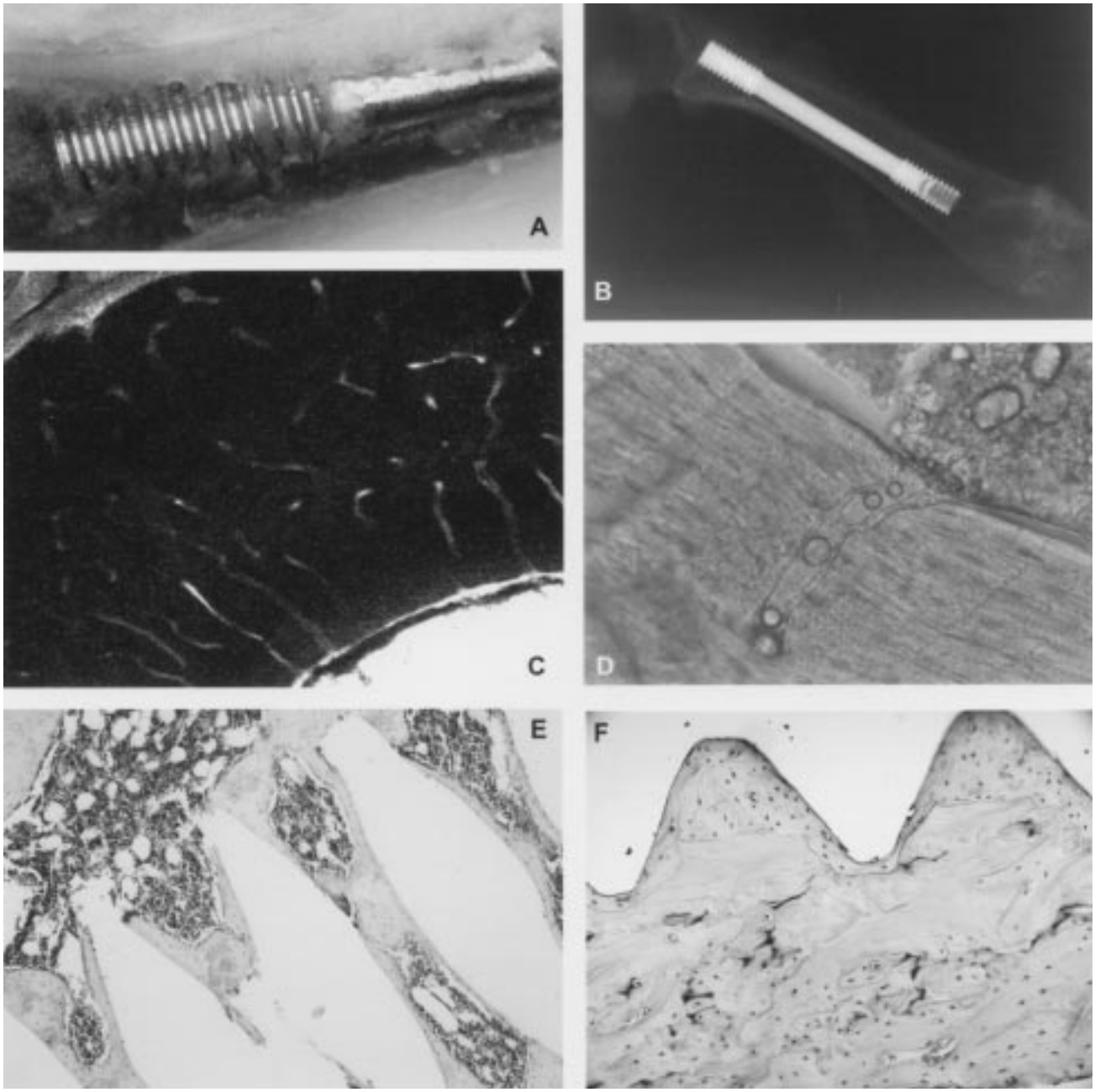

Figure 1.
a) Light micrograph of the proximal end of titanium fixture in rat femur. The femur was cut longitudinally after decalcification, and this has affected the integrity of the interface between bone and titanium. **b)** X-ray of fixture in rat femur 8 wk after insertion. Note threads on both ends of fixture, and hexagonal hole in distal end used to assist insertion of threaded fixture. **c)** Transverse, confocal microscopic image of rat femur 8 wk after insertion of titanium fixture. The fixture threads are not visible. PGP 9.5 antibody staining axons was labeled with fluorescent secondary antibody to visualize neural density in 60-um-thick sections. Note normal density of nerve fibers accompanying vascular space. Medullary cavity is seen at lower right. Original magnification 40x. **d)** Light micrograph using Nomarski phase optics of a transverse section of femur 8 wk after osseointegration demonstrates that there is normal vascular connection between the intramedullary cavity (top right) and bone. Original magnification 60x. **e)** Longitudinal section of rat femur after 8 wk of osseointegration. The fixture was removed after the tissue had been decalcified, revealing an active process of bone remodeling associated with the threads of the fixture. Section is stained with CGRP, indicating high density of CGRP-positive marrow cells participating in the remodeling process. Tissue counterstained with hematoxylin. Original magnification 20x. **f)** Nomarski phase micrograph of longitudinal section of rat femur 8 wk after implantation of titanium fixture. Note that bone remodeling has resulted in appearance of normal mature bone in threaded spaces of fixture (*). Original magnification 40x.

cavity was felt as a "loss of resistance." The position of the drill within the medullary cavity was checked by gently bending in circumferential directions to locate the walls of the medullary cavity. A defined drill depth of 27 mm was measured from the joint surface and corresponded to a mark on the drill. In cases of proximal drill resistance in smaller rats, a depth of 25 mm was considered sufficient.

A M2 pre-tapping device was inserted and the preformed medullary canal was tapped to the appropriate depth. The mid-section of the implant was grasped with titanium forceps and a 1.2-mm diameter Allen key was adapted to the corresponding hole. The implant was inserted, and countersunk 5 or 7 mm, in accordance with earlier measurements. After repositioning of the patella the wound was closed with 3-0 absorbable suture (Vicryl®, Ethicon, Germany) using continuous stitches in joint capsule and skin. To avoid post-surgical biting, the wound was sprayed with protection fluid (Op-Site®, Smith and Nephew, England). The animals were allowed immediate, unrestricted mobilization. During the first week after surgery clinical observation was made daily; thereafter, twice a week.

Tissue Collection and Processing

After 8 wk of healing, a time-point reflecting the anticipated period for unloaded titanium fixtures to become osseointegrated (9), the animals were anesthetized with the same procedure used for implant surgery. Thoracotomy was performed and a 2.0 mm diameter needle with blunt transverse edge was placed and fixed in the ascending aorta through the left cardiac ventricle. The right atrium was opened to allow drainage of blood from the vascular system. The rats were perfused with 350 ml Tyrodes Buffer, of which the first 175 ml were at room temperature and the remaining volume chilled to 4 ˚C. This was followed by perfusion with 350 ml of Zamboni's fixative.

Immediately after perfusion, both femurs were collected. The thigh was exposed through an extended lateral incision. Soft tissues were removed with preservation of the periosteum. After exarticulation of the knee and hip joints, the femurs were removed and all specimens were x-rayed using dental equipment. Femurs were immersed in Zamboni's fixative for an additional 48 hr before storage in phosphate-buffered saline and processing for histology.

A hydrated aluminum chloride solution (7 percent, w/v) with formic acid (5 percent, v/v), HCl (8.5 percent, v/v), and distilled water was used to decalcify the bone specimens. The bone became sufficiently soft after 2–3 d in this solution at 4 ˚C. Phosphate buffer rinse stopped the decalcification process.

Immunohistological Methods

Immunohistochemical studies were performed with antibodies to Protein Gene Product 9.5 (PGP 9.5), Calcitonin Gene-Related Peptide (CGRP), ED-1, and Growth-Associated Protein 43 (GAP-43) (**Table 1**). Sections for confocal microscopy were from either frozen or paraffin blocks and were 60 um thick; all other microscopy was done with 10-um-thick sections of paraffin-embedded decalcified bone. Processing included deparaffinization and rehydration with 70 percent ethanol. Antigen retrieval was facilitated by placement of the sections in DAKO Target Retrieval Solution (DAKO Corporation, Carpinteria, CA) for 10 min at 80–90 ˚C, followed by washing. Five percent blocking serum (goat) was applied for 5 min, with the excess blotted off the tissue. The primary antibody was applied in a dilution as indicated in **Table 1**, and incubated overnight at 4 ˚C in a humidified chamber. Negative controls used normal serum instead of primary antibody. Following rinse, a biotinylated antibody (goat anti-rabbit) was applied for 45 min. The Avidin-Biotin Complex (ABC) and chromagen

Table 1.
Antibodies

Antibodies	Manufacturer	Dilution	Target Tissue
PGP 9.5	Biogenesis	1:1K	Axoplasmic proteins in both myelinated and unmyelinated axons. A marker of axons.
CGRP	DiaSorin	1:1K	Calcitonin Gene-Related Petide. Constituent of small diameter sensory axons. Also neuropeptide involved in bone remodeling.
GAP-43	Sigma	1:1K	Growth-Associated Protein 43. Marker for sprouting axons.
ED-1	Serotec	1:1K	Marker for macrophages and monocytes.

(3,3'-diaminobenzidine; DAB) solutions were applied according to the manufacturers' recommendations (Vector Laboratories, Inc., Burlingame, CA). Finally, counterstaining with hematoxylin or methyl green was performed on some sections. Sections were cover-slipped.

Microscopy

The tissue was visualized by confocal, fluorescent, bright-field, and phase microscopy. A Zeiss LSM 510 confocal microscope from the VA Core Microscopy Laboratory was used to view thick sections of tissue. Light and fluorescent photomicroscopy was performed with a Leica DMR microscope system with Nomarski optics and a Polaroid DMC 1E digital camera connected to a Macintosh G4 imaging system with Adobe Photoshop software.

RESULTS

Animals and Implants

After implant insertion, slight initial limping was noticed in some animals, but no pronounced motion disorders were seen; neither were there signs of infection, failure to thrive, or other complications. At the time of sacrifice, a limited superficial reaction was noticed in all specimens at the femoral cartilage around the knee joint entrance. However, no major signs of osteoarthritis were seen. The length of the femur on the operated side was generally 2–3 mm shorter than the non-operated side.

X-rays of femoral specimens taken at 8 wk (**Figure 1b**) showed that all implants were within the medullary cavity. All femurs were intact. The proximal threads had an accurate cortical attachment except for one specimen where the threads had perforated the lateral aspect. No signs of resorption were seen. The distal threads were situated in the metaphysic region where the cortical diameter was significantly larger. No signs of radiologically detectable reactions were seen in this area.

Microscopy

The structure of bone surrounding the titanium implants appeared normal after 8 wk of intramedullary osseointegration. There were no significant inflammatory reactions, but there were obvious signs of bone remodeling adjacent to the proximal implant threads including changes in the size and shape of the bone (revealing the threads) and osteoclast activity resulting in new bone lamellae.

The density and structure of the vasculature in bone adjacent to the implants was qualitatively similar to that seen in unoperated contralateral femurs used for control. Confocal microscopy of PGP 9.5-stained experimental sections showed normal density and form of nerve fibers accompanying the vasculature 8 wk following osseointegration (**Figure 1c**), and normal medullary, and cortical bone anatomy (**Figure 1d**).

Light microscopy and phase microscopy of bone showed the active integration of titanium threads to remodeling bone (**Figures 1e,1f**), evidenced by changes in both structure and neuropeptide activity of activated bone marrow cells participating in the remodeling of bone around the threads. Bone adjacent to the threads was seen at 8 wk to have formed mature bone tissue (**Figure 1f**).

Immunohistochemical changes were especially striking for CGRP, which highlighted cells participating in bone remodeling and small sensory nerve fibers. The periosteum and surfaces of remodeling bone were lined with CGRP-positive cells in many instances (**Figures 2a,2b**) during what appeared to be an active period of remodeling. Staining was seen in higher density in areas where the remodeling process had not yet been finalized. Similarly, many bone marrow cells were positive for CGRP during the time of active bone remodeling (**Figures 2c,2d**). CGRP-positive nerve fibers were seen in both control and experimental sections of bone at approximately the same density, and they accompanied the vasculature (**Figures 2e,2f**). Given that there was some variability in both the control and experimental sections with respect to the positive identification and density of nerve fibers reactive to the CGRP antibody, additional quantitative studies were considered not to be productive. We suggest that the results reflect a similar degree of staining, given normal variance in biological methods. The same result pertained to studies with PGP 9.5 (**Figures 2e,2f**) and GAP-43 (not illustrated).

DISCUSSION

Osseointegration

Brånemark (1) has studied the processes of osseointegration for endosseous titanium implants in long bones under various conditions. Histological analysis indicated that all fixtures showed a direct bone contact with the titanium surface at the resolution level of the light microscope. The present results with intramedullary implants support these findings.

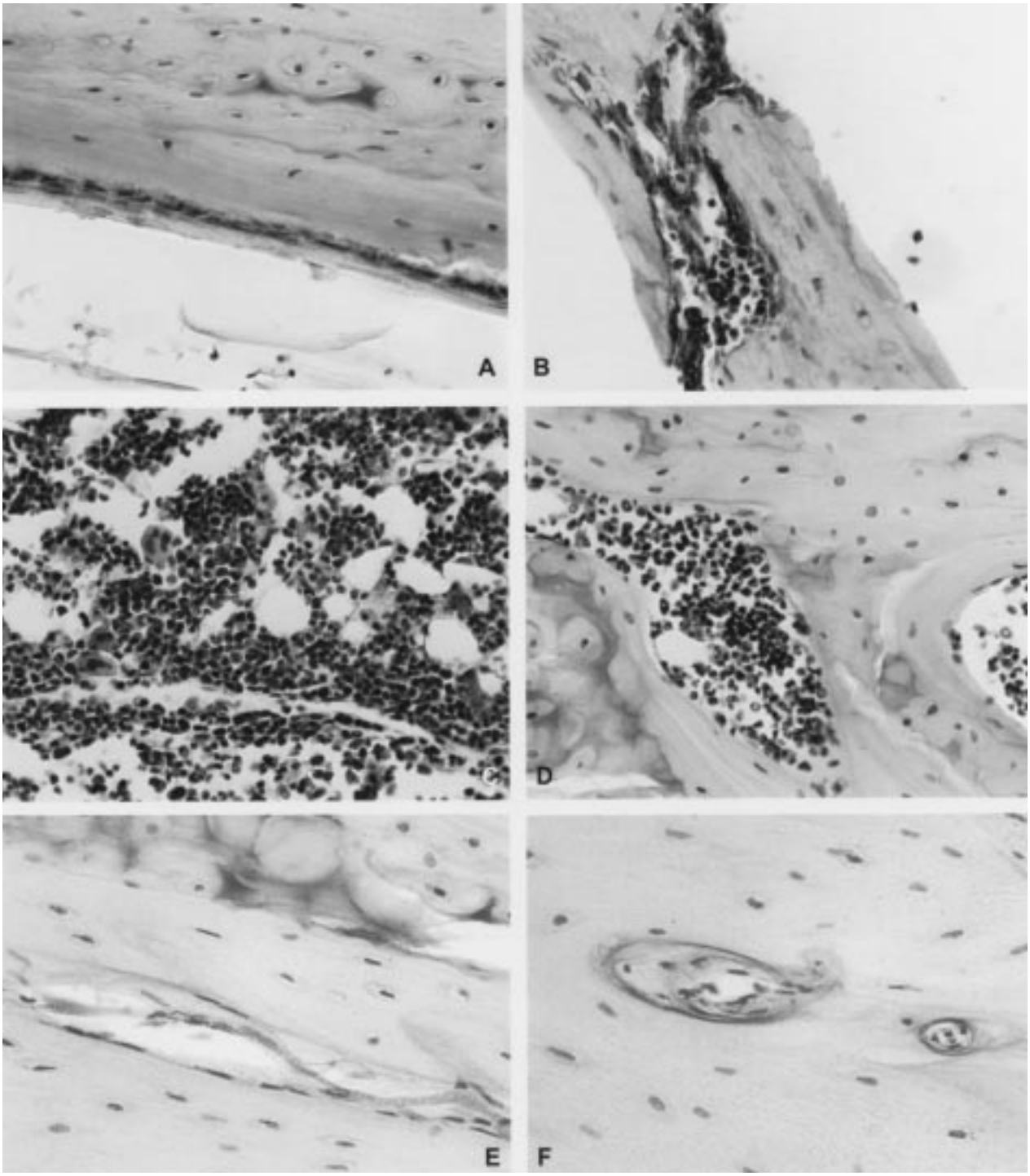

Figure 2.
a–d: CGRP immunohistochemistry of rat femur 8 wk after intramedullary implantation of titanium fixture. a) Note high density of CGRP-positive cells in cortical layer of bone (*). Original magnification 40x. b) CGRP-positive cells in marrow are seen in especially high density at the borders of bone actively being reformed adjacent to the titanium fixture. Original magnification 40x. c–d) Large, CGRP-positive cells in bone marrow reflecting activated monocytes/macrophages and osteoclasts were seen in higher density in remodeling bone (*) (c) than in normal bone taken from the femur contralateral to the one used for titanium implantation (d). Original magnifications 40x. e–f) PGP 9.5-positive axons (*) seen in longitudinal (e) and transverse (f) sections of rat femur 8 wk after titanium implantation. Note that the fibers are within vascular spaces. Original magnification 40x.

Neuropeptide Expression

The important relationship between the nervous system and bone is increasingly being recognized. Our exploration of the anatomical basis of osseoperception is only the most recent extension of this interest. It has been established previously that experimental denervation prior to fracture influences bone turnover (10) and that the neuropeptide CGRP influences osteoclastic bone resorption (11–14). Osteoclasts are derived from mononuclear, hematopoietic progenitor cells related to the monocyte/macrophage cell lineages. Their activity is increased by parathyroid hormone and decreased by calcitonin. Stimulation is controlled in part by osteoblast secretory factors and osteoclast activating factors including leukotrienes and prostaglandins. Increases in CGRP immunoreactivity have also been noted in association with bone remodeling following implantation of partially cemented fixtures in the tibia of goats (15). These authors noted accumulation of correlative data between extensive sprouting of CGRP-positive fibers and remodeling of necrotic endosteal bone, and suggested that sensory fibers have a regulatory role in angiogenesis and/or in bone remodeling. Our results expand these observations by illustrating the neuropeptide process in a new model of intramedullary osseointegration using experimental neuropathology methods.

The cellular biology of bone-resorbing cells has been explored in parallel studies of cytokine signaling and cellular immunology (16). The osteoclast has an important role in bone remodeling that is analogous to the role of macrophages in nerve injury and regeneration. In this context, we confirm that cellular concentration of CGRP increases in association with osseointegration. Bone marrow cells of the morphologic form resembling osteoclasts and activated monocytes or macrophages were CGRP-positive in higher density in osseointegrated specimens. Since osteoclasts are considered to arise from the fusion of cells in the mononuclear phagocyte system, it is reasonable to expect that both mononuclear cells and osteoclasts express CGRP. While the exact functional relationship between neuropeptides and bone remodeling remains to be clarified, this work establishes an experimental model that may be useful in exploring the relationships between bone injury, neuropeptides, pain, and bone remodeling.

Sensory Innervation of Bone

Innervation of bone was reported in 1945 (17), but has only been studied in detail since the 1980s when immunohistochemical techniques became available (18–24). Immunohistochemistry has shown that there are nerve fibers in skeleton that are immuno-positive for substance P, CGRP, neuropeptide Y, Vasoactive Intestinal Protein (VIP), tyrosine hydroxylase, and met-enkephalin. As reviewed by Buma, Elmans, and Oestreicher (15), it is currently thought that the fibers arise from both dorsal root ganglia of the sensory nervous system and sympathetic ganglia of the autonomic system, and that these fibers have more than one function. Based on the chemical and structural relationships between the fibers and adjacent tissues, it is concluded that pain and proprioception are mediated by a subset of these fibers, while some fibers are probably involved with efferent regulation of the circulation and/or osteoclast function.

Our results support these findings by demonstrating active growth of small, PGP-positive nerve fibers in remodeled bone adjacent to the fixtures. Intramedullary innervation in rat femur is provided by sensory fibers at the L2–L5 dorsal root ganglia (DRG) level, with a more variable contribution by L2–L5 paravertebral sympathetic ganglia (Nakamura and Myers, unpublished observations). We originally proposed the hypothesis that osseoperception was a sensory phenomenon mediated in part by an increased number of CGRP/PGP-positive fibers developing adjacent to osseointegrated fixtures. However, after 8 wk of osseointegration, extensive qualitative analysis of immunohistologically stained specimens revealed that there was no substantial difference in the innervation of bone when compared to the contralateral control tissue. Changes may have occurred outside the time period of our study or the methods used were not sensitive enough to reveal small changes in nerve density and/or activity. Insertion of the fixtures may not have caused significant bone necrosis, a factor known to stimulate nerve fiber sprouting (15). Loading of the implants, as seen in the clinical situation, could also be of importance. Current research activities are focused on this issue.

CONCLUSION

We conclude that the rat model described herein results in osseointegration of an intramedullary titanium device in 8 wk that is surrounded by normal bone. Continued experimental study of intramedullary osseointegration is planned to extend these results and support future applications of osseointegration and osseoperception in orthopedics.

REFERENCES

1. Brånemark R. A biomechanical study of osseointegration. *In-vivo* measurements in rat, rabbit, dog and man [dissertation]. Gothenburg, Sweden: Gothenburg University; 1996. ISBN 91-628-2267-5.
2. Ferguson ABJ. Historical use of metals in the human body. In: Bechtol CO, Ferguson ABJ, Laing PG, editors. Engineering bone and joint surgery. Baltimore: Williams and Wilkins Company; 1959. p. 1–18.
3. Brånemark P-I, Hansson BO, Adell R, Breine U, Lindström J, Öhman A. Osseointegrated implants in the treatment of the edentulous jaw. Experience from a 10-year period. Stockholm: Almqvist & Wiksell International; 1977.
4. Brånemark P-I, Rydevik BL, Skalak R, editors. Osseointegration in skeletal reconstruction and joint replacement. Proceedings of the Second International Workshop on Osseointegration in Skeletal Reconstruction and Joint Replacement, Rancho Sante Fe, California, October 27-29 1994. Quintessence Publishing Co., Inc., 1997; London.
5. Adell R, Eriksson B, Lekholm U, Brånemark P-I, Jemt T. A long-term follow-up study of osseointegrated implants in the treatment of the totally edentulous jaw. Int J Oral Maxillofac Implants 1990;5:347–59.
6. Esposito M, Hirsch J-M, Lekholm U, Thomsen P. Biological factors contributing to failures of osseointegrated oral implants. (I) Success criteria and epidemiology. Eur J Oral Sci 1998;106:527–51.
7. Worthington P. History, development, and current status of osseointegration as revealed by experience in craniomaxillofacial surgery. In: Brånemark PI, Rydevik BL, Skalak R, editors. Osseointegration in skeletal reconstruction and joint replacement. London: Guintessence Books; 1997. p. 25–44.
8. Rydevik BL. Amputation prostheses and osseoperception in the lower and upper extremity. In: Brånemark P-I, Rydevik BL, Skalak R, editors. Osseointegration in skeletal reconstruction and joint replacement. London: Guintessence Books; 1997. p. 175–82.
9. Brånemark R, Öhrnell L-O, Nilsson P, Thomsen P. Biomechanical characterization of osseointegration during healing. An experimental *in-vivo* study in the rat. Scand J Plast Reconstr Surg Hand Surg 1997;31:281–93.
10. Madsen JE, Aune AK, Falch JA, Hukkanen M, Konttinen YT, Santavirta S, Nordsletten L. Neural involvement in post-traumatic osteopenia: an experimental study in the rat. Bone 1996;18:411–6.
11. D'Souza SM, MacIntyre I, Girgis SI, Mundy GR. Human synthetic calcitonin gene-related peptide inhibits bone resorption in vitro. Endocrinology 1986;119:58–61.
12. Konttinen YT, Imai S, Suda A. Neuropeptides and the puzzle of bone remodeling. State of the art. Acta Orthop Scand 1996;67:632–9.
13. Zaidi M, Chambers TJ, GainesDas RE, Morris HE, MacIntyre I. A direct action of human calcitonin gene-related peptide on isolated osteoclasts. J Endocrinol 1987;115:511–8.
14. Zaidi M, Fuller K, Bevis PJR, GainesDas RE, Chambers TJ, MacIntyre I. Calcitonin gene-related peptide inhibits osteoclastic bone resorption: a comparative study. Calcif Tissue Int 1987;40:149–54.
15. Buma P, Elmans L, Oestreicher AB. Changes in innervation of long bones after insertion of an implant: immunocytochemical study in goats with antibodies to calcitonin gene-related peptide and B-50/GAP-43. J Orthop Res 1995;13:570–7.
16. Athanasou NA. Current concepts review: cellular biology of bone-resorbing cells. J Bone Joint Surg Am 1996;78:1096–112.
17. Kuntz A, Richings CA. Innervation of the bone marrow. J Comp Neurol 1945;83:213–22.
18. Gronblad M, Liesi P, Korkala O, Karaharju E, Polak J. Innervation of human bone periosteum by peptidergic nerves. Anat Rec 1984;209:297–9.
19. Hohmann EL, Elde RP, Rysavy JA, Einzig S, Gebhard RL. Innervation of periosteum and bone by sympathetic vasoactive intestinal peptide-containing nerve fibers. Science 1986;232:868–71.
20. Bjurholm A, Kreicbergs A, Brodin E, Schultzberg M. Substance P- and CGRP-immunoreactive nerves in bone. Peptides 1988;9:165–71.
21. Bjurholm A, Kreicbergs A, Terenius L, Goldstein M, Schultzberg M. Neuropeptide Y-, tyrosine hydroxylase- and vasoactive intestinal polypeptide-immunoreactive nerves in bone and surrounding tissues. J Auton Nerv Syst 1988;25:119–25.
22. Cavanaugh JM, El-Bohy A, Hardy WN, Getchell TV, Getchell ML, King AI. Sensory innervation of soft tissues of the lumbar spine in the rat. J Orthop Res 1989;7:378–88.
23. Kruger L, Silverman JD, Mantyh PW, Sternini C, Brecha NC. Peripheral patterns of calcitonin-gene-related peptide general somatic sensory innervation: cutaneous and deep terminations. J Comp Neurol 1989;280:291–300.
24. Hill EL, Elde R. Distribution of CGRP-, VIP-, DBH-, SP- and NPY-immunoreactive nerves in the periosteum of the rat. Cell Tissue Res 1991;264:469–80.

Submitted for publication July 11, 2000. Accepted in revised form November 14, 2000.